

# Radiation of non-relativistic particle on a conducting sphere and a string of spheres

N.F. Shul'ga<sup>a</sup>, V.V. Syshchenko<sup>b,\*</sup>, E.A. Larikova<sup>b</sup>

<sup>a</sup>*A.I. Akhiezer Institute for Theoretical Physics, NSC “KIPIT”,  
Akademicheskaya Street, 1, Kharkov 61108, Ukraine*

<sup>b</sup>*Belgorod State University, Pobedy Street, 85, Belgorod 308015, Russian Federation*

---

## Abstract

The radiation arising under uniform motion of non-relativistic charged particle by (or through) perfectly conductiong sphere is considered. The rigorous results are obtained using the method of images known from electrostatics.

*Keywords:* Transition radiation, Diffraction radiation, Conducting sphere, Method of images

---

## 1. Introduction

The radiation emitting under charged particle crossing the boundary between two media with different electrodynamic properties is known as transition radiation (TR), whereas for the particle traveling near the boundary of the spatially localized target without crossing the emitting radiation is called as diffraction radiation (DR). DR and TR of a charge on a perfectly conducting sphere (as well as on a periodic string of the spheres) are studied in the present paper.

Various aspects of DR and TR on spherical targets had been considered in numerous papers, see, e.g., [1]–[4]. However, these papers either deal with some special cases or present the result in rather complicated form. Here we propose the simple and economic method for computation of the radiation characteristics (spectral-angular density as well as polarization, if needed) based on the following idea.

---

\*Corresponding author. Tel.: +7 4722 301819; fax: +7 4722 301012  
Email address: [sysch@yandex.ru](mailto:sysch@yandex.ru) (V.V. Syshchenko)

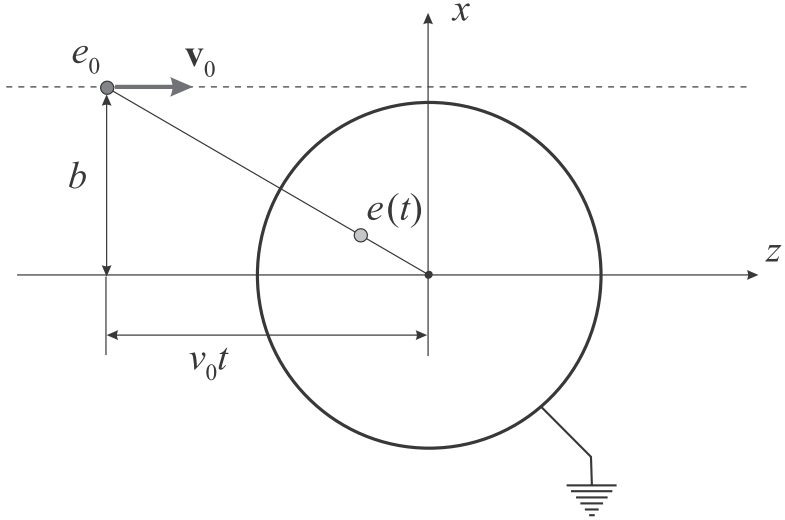


Figure 1: Positions of the real charge  $e_0$  and its “image”  $e(t)$  near grounded conducting sphere of the radius  $R$ .

One of the ways to describe these types of radiation is the application of the boundary conditions to the Maxwell equations solutions for the field of the moving particle in two media. It becomes evident that the boundary conditions could be satisfied only after addition the solution of free Maxwell equations that corresponds to the radiation field, see, e.g. [5].

The conditions on the boundary between vacuum and ideal conductor could be satisfied in some cases via introduction of one or more fictive charges along with the real charged particle; this approach to electrostatic problems is known as the method of images, see, e.g., [6]. Namely the method of images had been used in the pioneering paper [7] where TR on a metal plane had been predicted. The method of images had been used also in [8] for consideration of TR under passage of the particle through the center of the ideally conducting sphere in dipole approximation.

## 2. DR on sphere

Consider the real charge  $e_0$  passing by the grounded conducting sphere of the radius  $R$  with the constant velocity  $v_0 \ll c$ , see Fig. 1. Its image of

the magnitude

$$e(t) = -e_0 \frac{R}{\sqrt{b^2 + v_0^2 t^2}}, \quad (1)$$

has to be placed in the point with coordinates

$$x(t) = \frac{R^2 b}{b^2 + v_0^2 t^2}, \quad z(t) = \frac{R^2 v_0 t}{b^2 + v_0^2 t^2}. \quad (2)$$

So, while the incident particle moves uniformly, its “image” will move accelerated,

$$v_x = \frac{dx}{dt} = -\frac{2R^2 b v_0^2 t}{(b^2 + v_0^2 t^2)^2}, \quad v_z = \frac{dz}{dt} = \frac{R^2 v_0 (b^2 - v_0^2 t^2)}{(b^2 + v_0^2 t^2)^2}. \quad (3)$$

The radiation produced by non-uniform motion of the fictive charge will be described by well-known formula [9]

$$\frac{d\mathcal{E}}{d\omega d\Omega} = \frac{1}{4\pi^2 c} |\mathbf{k} \times \mathbf{I}|^2, \quad (4)$$

where  $\mathbf{k}$  is the wave vector of the radiated wave,  $|\mathbf{k}| = \omega/c$ , and

$$\mathbf{I} = \int_{-\infty}^{\infty} e(t) \mathbf{v}(t) e^{i(\omega t - \mathbf{k} \cdot \mathbf{r}(t))} dt \quad (5)$$

(it could be easily seen that it is applicable to the case of time-varying charge  $e(t)$  as well as to the case of the constant one). Note that the method of images for the isolated (in contrast to grounded) sphere requires introducing another fictive charge of the magnitude  $-e(t)$  resting in the center of the sphere. However, the last equation shows that such rest charge does not produce any radiation.

Substitution of (1), (2), (3) into (5) gives the following integrals:

$$\begin{aligned} I_x &= 2e_0 b R^3 v_0^2 \times \\ &\times \int_{-\infty}^{\infty} \exp \left\{ i \left[ \omega t - \frac{k_x R^2 b}{b^2 + v_0^2 t^2} - \frac{k_z R^2 v_0 t}{b^2 + v_0^2 t^2} \right] \right\} \frac{t dt}{(b^2 + v_0^2 t^2)^{5/2}}, \\ I_z &= -e_0 R^3 v_0 \times \\ &\times \int_{-\infty}^{\infty} \exp \left\{ i \left[ \omega t - \frac{k_x R^2 b}{b^2 + v_0^2 t^2} - \frac{k_z R^2 v_0 t}{b^2 + v_0^2 t^2} \right] \right\} \frac{(b^2 - v_0^2 t^2) dt}{(b^2 + v_0^2 t^2)^{5/2}}. \end{aligned} \quad (7)$$

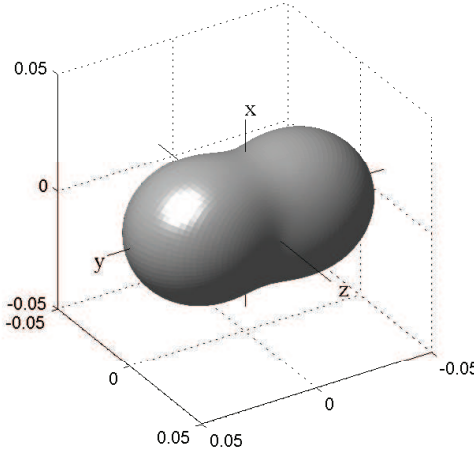


Figure 2: The angular dependence of DR intensity as direction diagram for the passage of the real charge under  $b = R$  (sliding incidence on the sphere, when DR intensity is maximal for the whole range of wavelengths) and  $R\omega/v_0 = 2.34$  (this choice is due to the maximum of DR spectrum (see below) falls on  $b\omega/v_0 \approx 2.34$  and  $b = R$  in the given case).

The integration in (6), (7) can be easily performed numerically, that leads to the spectral-angular density of diffraction radiation in the form

$$\frac{d\mathcal{E}}{d\omega d\Omega} = \frac{e_0^2}{4\pi^2 c} \Phi_{DR}(\theta, \varphi, \omega), \quad (8)$$

where the typical shape of the angular distribution  $\Phi_{DR}(\theta, \varphi, \omega)$  is presented in Fig. 2; for different values of parameters it do not vary too much.

Approximative analytical result can be obtained after neglecting the second term in the exponents in (6), (7) (that is valid for low radiation frequencies,  $\omega \ll cb/R^2$ ) as well as the third term (that is always valid for non-relativistic case):

$$\begin{aligned} \frac{d\mathcal{E}}{d\omega d\Omega} = & \frac{e_0^2}{4\pi^2 c} \frac{16R^6\omega^6}{9c^2v_0^4} \left\{ (1 - \sin^2 \theta \cos^2 \varphi) K_1^2 \left( \frac{\omega}{v_0} b \right) + \right. \\ & \left. + \sin^2 \theta \left( \frac{v_0}{2\omega b} \right)^2 \left[ K_1 \left( \frac{\omega}{v_0} b \right) + 2 \frac{\omega}{v_0} b K_0 \left( \frac{\omega}{v_0} b \right) \right]^2 \right\}. \end{aligned} \quad (9)$$

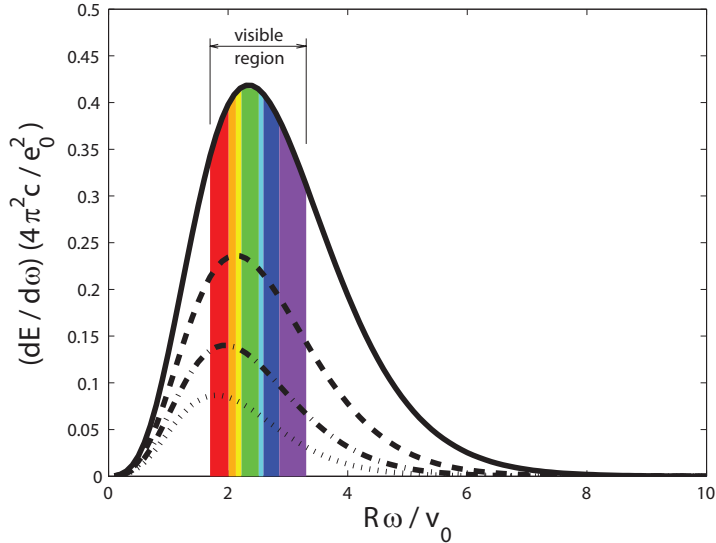


Figure 3: DR spectrum for  $R = 20$  nm,  $v_0 = 0.1c$  and  $b = R$  (solid line),  $b = 1.1R$  (dashed line),  $b = 1.2R$  (dash-dotted line),  $b = 1.3R$  (dotted line).

Integration of (8) over radiation angles leads to the radiation spectrum presented in Fig. 3. For illustrative purposes, we choose the parameters  $v_0 = 0.1c$ ,  $R = 20$  nm,  $b = R + 0$ , for which the DR intensity maximum will lie in the visible spectrum. Note, however, that in this frequency domain the properties of the sphere material can be far from that of a perfect conductor. Particularly, plasma oscillations can be important.

### 3. DR on the string of spheres

Now consider the particle  $e_0$  motion along the periodic string of  $N \gg 1$  spheres. The mutual influence of the fictive charges induced in the neighboring spheres can be neglected in the case of small impact parameters,  $b \rightarrow R$  (when the radiation intensity is high), for the string period large enough,  $a \gtrsim 5R$ . Then the interference of the radiation produced on the subsequent spheres leads to the simple formula for the spectral-angular density of DR:

$$\frac{d\mathcal{E}}{d\omega d\Omega} = \frac{e_0^2}{4\pi^2 c} \Phi_{DR}(\theta, \varphi, \omega) \times \quad (10)$$

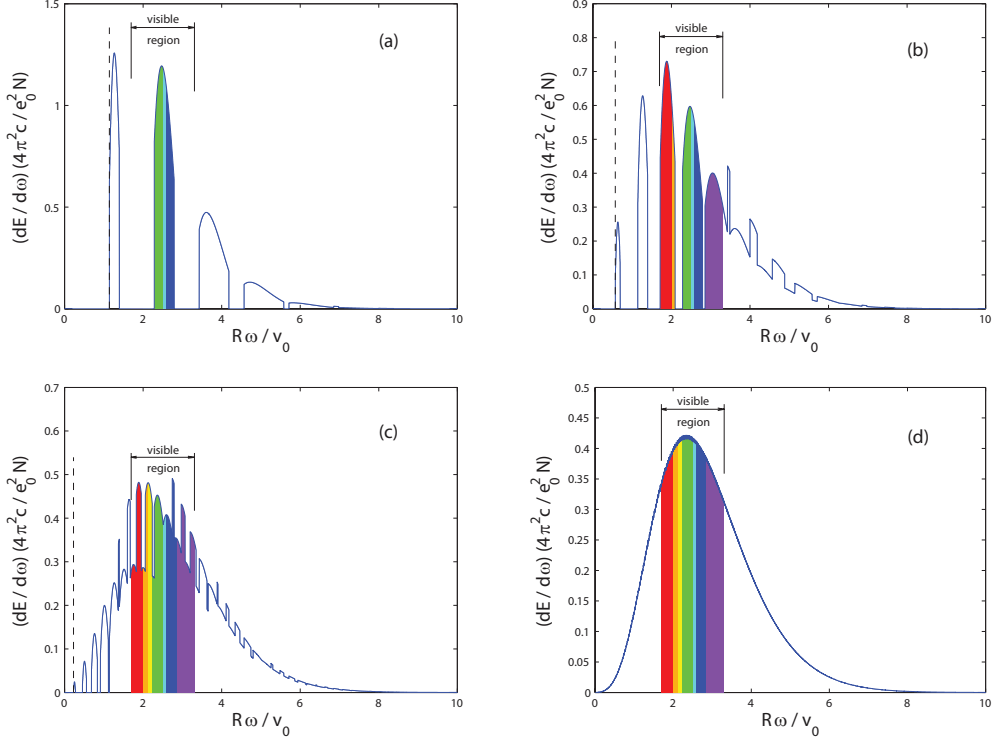


Figure 4: DR spectrum on the string of spheres under  $b = R$ ,  $R = 20$  nm,  $v_0 = 0.1c$ ,  $a = 100, 200, 500, 20000$  nm. Vertical dashed line marks the long wavelength edge of the spectrum.

$$\times 2\pi N \frac{v_0}{\omega a} \sum_{m=1}^{\infty} \delta \left( 1 - \frac{v_0}{c} \cos \theta - m \frac{2\pi v_0}{\omega a} \right),$$

where the delta-function means well-known Smith-Purcell condition [10].

The spectrum for the string period  $a$  small enough consists of separated bands, see Fig. 4, a. The bands overlap each other under increase of the string period  $a$  gradually forming the spectrum of DR on a single sphere (multiplied by the total number of the spheres  $N$ ), see Fig. 4, b, c, d.

#### 4. TR on the sphere

TR arises under  $b < R$ , when the incident charge  $e_0$  crosses the sphere. In this case both real and fictive charges vanish while crossing the sphere (and

then appear again) that complicates the formulae describing the radiation. For the convenience of the further interpretation, let us separate the contributions into the vector  $\mathbf{I}$  (5) from the real particle and its image on the time interval  $-\infty < t \leq -t_0$ , where  $t_0 = \sqrt{R^2 - b^2}/v_0$ , that is on the incoming part of the particle's trajectory,

$$I_z^{(real.in)} = 2ie_0v_0 \frac{\exp[-ik_xb + i(\omega - k_zv_0)t_0]}{\omega - k_zv_0}, \quad (11)$$

$$\begin{aligned} I_x^{(image.in)} &= 2e_0bR^3v_0^2 \times \\ &\times \int_{-\infty}^{-t_0} \exp \left\{ i \left[ \omega t - \frac{k_xR^2b}{b^2 + v_0^2t^2} - \frac{k_zR^2v_0t}{b^2 + v_0^2t^2} \right] \right\} \frac{t dt}{(b^2 + v_0^2t^2)^{5/2}}, \\ I_z^{(image.in)} &= -e_0R^3v_0 \times \\ &\times \int_{-\infty}^{-t_0} \exp \left\{ i \left[ \omega t - \frac{k_xR^2b}{b^2 + v_0^2t^2} - \frac{k_zR^2v_0t}{b^2 + v_0^2t^2} \right] \right\} \frac{(b^2 - v_0^2t^2) dt}{(b^2 + v_0^2t^2)^{5/2}}, \end{aligned} \quad (13)$$

and on the interval  $t_0 \leq t < \infty$ , that is on the outgoing part of the particle's trajectory,

$$I_z^{(real.out)} = -2ie_0v_0 \frac{\exp[-ik_xb - i(\omega - k_zv_0)t_0]}{\omega - k_zv_0}, \quad (14)$$

$$\begin{aligned} I_x^{(image.out)} &= 2e_0bR^3v_0^2 \times \\ &\times \int_{t_0}^{\infty} \exp \left\{ i \left[ \omega t - \frac{k_xR^2b}{b^2 + v_0^2t^2} - \frac{k_zR^2v_0t}{b^2 + v_0^2t^2} \right] \right\} \frac{t dt}{(b^2 + v_0^2t^2)^{5/2}}, \\ I_z^{(image.out)} &= -e_0R^3v_0 \times \\ &\times \int_{t_0}^{\infty} \exp \left\{ i \left[ \omega t - \frac{k_xR^2b}{b^2 + v_0^2t^2} - \frac{k_zR^2v_0t}{b^2 + v_0^2t^2} \right] \right\} \frac{(b^2 - v_0^2t^2) dt}{(b^2 + v_0^2t^2)^{5/2}}. \end{aligned} \quad (16)$$

Numerical integration leads to the spectral-angular density of transition radiation in the form

$$\frac{d\mathcal{E}}{d\omega d\Omega} = \frac{e_0^2}{4\pi^2 c} \Phi_{TR}(\theta, \varphi, \omega), \quad (17)$$

where the function  $\Phi_{TR}(\theta, \varphi, \omega)$  is presented for some particular cases as the directional diagram in Fig. 5. We see very sophisticate shapes in contrast

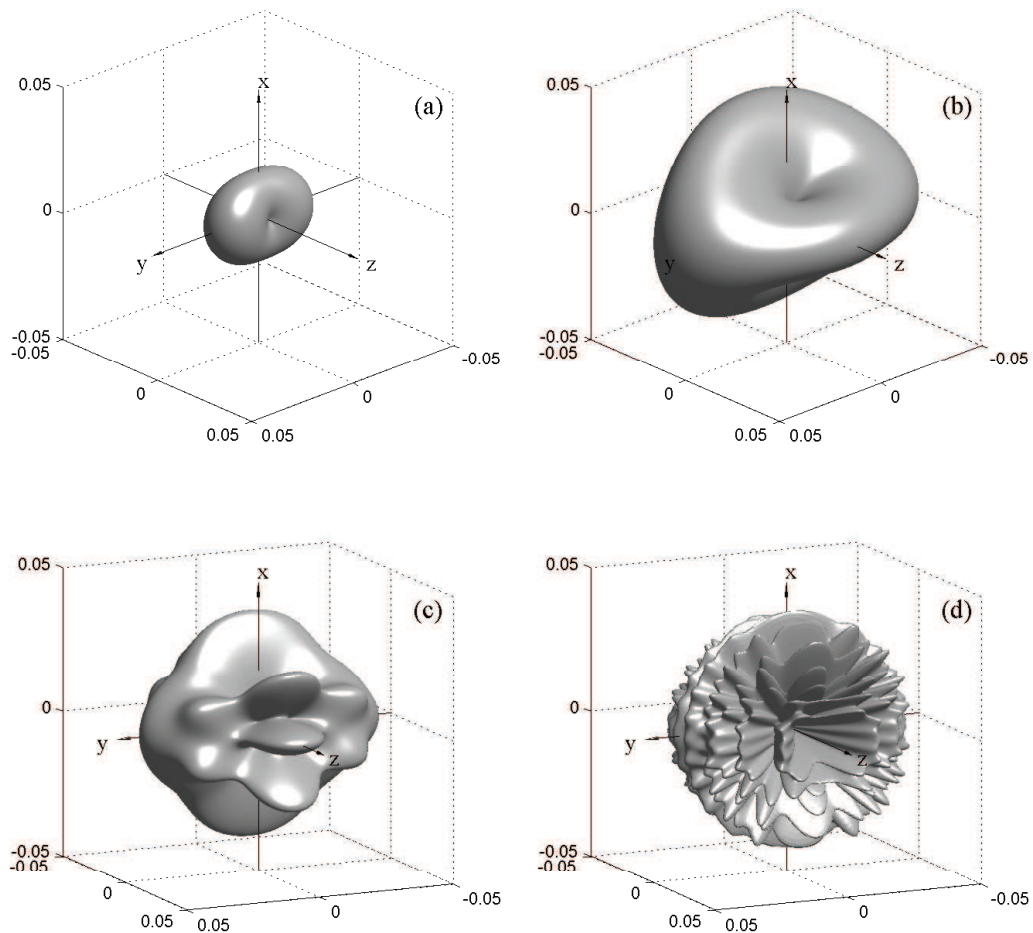


Figure 5: Direction diagrams of the radiation emitted under incidence of the real charge under  $b = R/\sqrt{2}$  for  $v_0 = 0.1c$ ,  $R\omega/v_0 = 1, 10, 50, 200$ .

to DR case. This is due to interference of the radiation emitted by the real charge and its image while crossing two boundaries between vacuum and conductor.

Let us trace out the origin of this interference picture in the case of high radiation frequency  $R\omega/v_0 \gg 1$ , when the transverse size of the particle's Coulomb field Fourier component is small and the curvature of the conductor surface is negligible. The elementary contributions from both real and fictive charges into the radiation under each crossing of the metal surface have similar shape with axis of symmetry along their velocity. So, for the real particle the axis of symmetry is directed along the  $z$  axis, see Fig. 6, a, where the directional diagram computed with the vector  $\mathbf{I}^{(real.in)}$  (11) or  $\mathbf{I}^{(real.out)}$  (14) instead of complete vector  $\mathbf{I}$  is presented. The interference of two such contributions from the enter point of the charge into the sphere and from the exit one leads to the directional diagram in the Fig. 6, b.

On the other hand, the axis of symmetry of the elementary contribution from the fictive charge for  $b = R/\sqrt{2}$  (that is for the incidence under 45 degrees) will be directed along the  $x$  axis (Fig. 6, c, which is computed for the vector  $\mathbf{I}^{(image.in)}$  (12), (13) or  $\mathbf{I}^{(image.out)}$  (15), (16)). The interference of two such contributions from two points of crossing the sphere leads to the picture in the Fig. 6, d.

At last, the interference of the contributions from the real charge (Fig. 6, b) and its image (Fig. 6, d) leads to the final picture of the radiation emission (Fig. 5, d).

TR spectrum

$$\frac{d\mathcal{E}}{d\omega} = \frac{e_0^2}{4\pi^2 c} \int \Phi_{TR}(\theta, \varphi, \omega) d\Omega \quad (18)$$

for  $b = R/\sqrt{2}$  is presented in Fig. 7.

## 5. Conclusion

The radiation emitting under interaction of non-relativistic particle with ideally conducting sphere is considered.

The method of images leads to precise description of the radiation in this case. The integration in the resulting formulae can be easily performed numerically.

When the incident particle crosses the sphere, the angular distribution of the radiation can be very complex. This is due to the interference of the

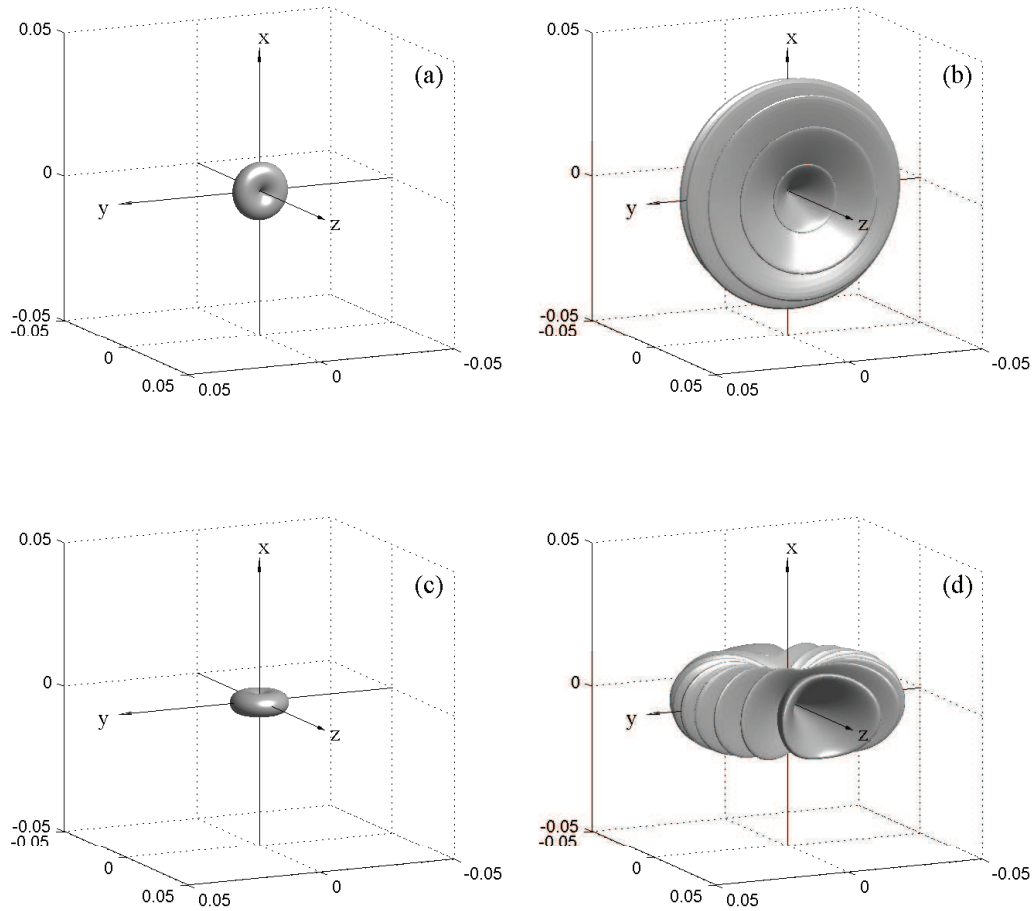


Figure 6: Direction diagrams of the partial contributions to the radiation emitted under incidence of the real charge under  $b = R/\sqrt{2}$  for  $R\omega/v_0 = 200$ ,  $v_0 = 0.1c$ .

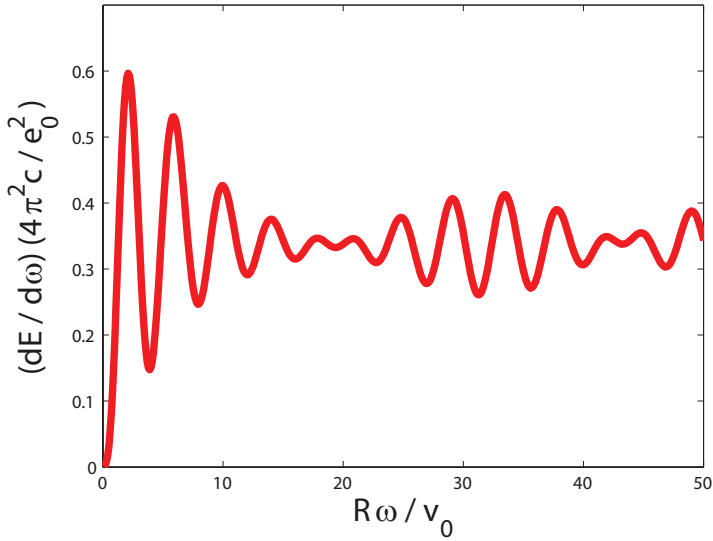


Figure 7: TR spectrum (18) for  $b = R/\sqrt{2}$ ,  $v_0 = 0.1c$ .

waves emitted by the particle and its image under crossing the boundaries between conductor and vacuum.

## 6. Acknowledgements

The work was supported by the Ministry of Education and Science of the Russian Federation (the State assignment N 3.500.2014/K).

## References

- [1] F.G. García de Abajo, Phys. Rev. E 61 (2000) 5743.
- [2] N.F. Shulga, S.N. Dobrovolsky, V.V. Syshchenko, Russian Physics Journal 44, No. 3 (2001) 317.
- [3] K.V. Lekomtsev, M.N. Strikhanov, A.A. Tishchenko, Journal of Physics: Conference Series 236 (2010) 012023.
- [4] V.A. Astapenko, S.V. Sakhno, Yu.A. Krotov, Journal of Physics: Conference Series 732 (2016) 012025.

- [5] M.L. Ter-Mikaelian, High-energy Electromagnetic Processes in Condensed Media, Wiley, New York, 1972.
- [6] J.D. Jackson, Classical Electrodynamics, Wiley, New York, 1999.
- [7] V.L. Ginzburg, I.M. Frank, J. Phys. USSR 9 (1945) 353.
- [8] G.A. Askaryan, JETP 29 (1955) 388 (in Russian).
- [9] A.I. Akhiezer, N.F. Shul'ga, High-Energy Electrodynamics in Matter, Gordon and Breach, 1996.
- [10] S.J. Smith, E.M. Purcell, Phys. Rev. 92 (1953) 1069.